Turkish Journal of Civil Engineering, 2023, 1-28, Paper 749, ***Research Article***

Hazard Curves for Reliability Assessment of Strip Footings on Spatially Varying Cohesive Soils

Ahmet Can MERT[1*]
Gökhan YAZICI[2]
Hadi KHANBABAZADEH[3]

ABSTRACT

The present study aimed to create a series of hazard curves against maximum total settlement and angular rotation of strip footings for probabilistic shallow foundation design on clays. Random field finite element method (RFEM) was adopted with elasto-plastic clay-like soil behavior, deformation modulus (E_d) and shear strength parameters (c and ϕ) were employed as random field inputs. Parameters were defined and assigned to the analysis models with varying correlation lengths (θ_h, θ_v). Models have been iteratively solved one thousand times, and output distributions of maximum settlement and angular rotations were recorded. Probability density functions (PDF) were fitted to the outputs, and probability of failure (P_f) for footing deformation limits was subsequently estimated. Proposed hazard curves for two anisotropy and three variability categories were developed employing the estimated P_fs. The method proposed has been validated using an independent database of in-situ results, and a worked example was provided to illustrate the implementation of the process. The key contribution of the research is to form hazard curves for shallow foundations considering elasto-plastic soil behavior with the impact of all influencing parameters, respecting the limit values for foundation deformation in the design codes. The proposed technique offers a probabilistic evaluation of strip footings with spatial variation of clayey soils and a valid method for the reliability-based design of foundations in the serviceability limit state.

Keywords: Random field finite element method, strip footings, soil-foundation-structure interaction, reliability-based design, serviceability limit state, cohesive soils.

Note:
- This paper was received on November 14, 2022 and accepted for publication by the Editorial Board on August 4, 2023.
- Discussions on this paper will be accepted by January 31, 2024.
- https://doi.org/10.18400/tjce.1340360

1 Bahcehesir University, Department of Civil Engineering, Istanbul, Türkiye
ahmetcan.mert@bau.edu.tr - https://orcid.org/0000-0002-2483-1330

2 Istanbul University Cerrahpasa, Department of Civil Engineering, Istanbul, Türkiye
gokhan.yazici@iuc.edu.tr - https://orcid.org/0000-0002-6719-9152

3 Gebze Technical University, Department of Civil Engineering, Kocaeli, Türkiye
hk.babazadeh@gtu.edu.tr - https://orcid.org/0000-0001-9764-7799

* Corresponding author

1. INTRODUCTION

Strip footings are simple yet effective superficial foundation systems, making them one of the initial alternatives to the design process. In most cases, strip footings fail by exceeding the serviceability limits (SLS) before reaching the ultimate limit state (ULS). Accordingly, the SLS governs the design rather than ULS in practice. Hence, many design regulations recommend deformation limits for footing design by SLS. For example, Eurocode 7 suggests a 25 mm maximum settlement for the serviceability limit of strip footings [1]. Regardless of the limit state considered, the primary factor for a sound foundation design is the determination of the soil parameters which accurately represent the site conditions. Any geotechnical solution may have three sources of uncertainties within this context: inherent soil variability, measurement error, and transformation uncertainty [2,3]. Measurement error and transformation uncertainty can be minimized by increasing the number of samples and using highly correlated equations. The inherent soil variability, the principal source of uncertainty, must be considered through probabilistic methods. Suitably, engineering codes such as Eurocode and ISO (International Organization for Standardization) accept the Reliability-Based Design (RBD) approach, representing the geotechnical parameter variation as a random variable fitting a probability distribution [4,5]. Reliability index (β) is the primary measure for RBD, and the design regulations recommend a target value β to achieve a reliable foundation design.

One of the practical tools to express the soil spatial variability is random field (RF) theory, which seeks to model complex patterns of variation and interdependence in cases where deterministic treatment is inefficient and conventional statistics are insufficient [6,7]. The first geotechnical application combined the random field theory with the finite element method on a footing settlement analysis using Taylor series expansion, entitled the stochastic finite element method (SFEM)[8]. Since the series expansion requires complex mathematical solutions, a practical alternative named the random field finite element method (RFEM) was developed, which preserves the probability distribution of deformation by iteratively solving random field realizations. The study conducted by Griffiths and Fenton in 2009 revealed that RFEM provides more reliable results than SFEM, especially in higher-order spatial variation [9]. RFEM can be applied to most shallow foundation problems, including the analysis of maximum settlement of strip footing [10–12], differential settlement of two strip footings in plain strain condition [13,14], maximum and differential settlement analysis of spread footings by RFEM in 3D [11,14]. There were further investigations on shallow foundation analysis by RFEM with eccentric and inclined loading cases [15,16]. These studies disclosed the need for soil uncertainty for foundation design, as soil spatial variability substantially affects failure modes and bearing capacity of shallow foundations [17,18]. From this point of view, the design of strip footings by deterministic methods leads to an over- or under-design compared to the RBD of footings. Thus, all related previous studies emphasized the significance of soil spatial variability.

Recent studies investigated the deformations of shallow foundations on elastic soil [19–22]. These works well represented the soil spatial variability, albeit the actual stress-strain behavior of soil can be overlooked due to the elastic conditions. The research on the nonlinear behavior of soil utilized Mohr-Coulomb (MC) failure criterion with Young's Modulus (E) random field for deformation analysis of single strip footing [10,23] and differential settlement analysis of two neighboring strip footings [13]. However, the studies solved the

problem with a single random variable. Another study considered the nonlinear soil behavior by MC failure criterion and employed Poisson's ratio ν as a random field in addition to Young's Modulus E [15]. A study by the first author performed RFEM in a 2D strip footing problem with CPT-based RF of soil deformation modulus (E_d), considering MC failure criterion [24]. Regardless of the number of parameters employed, footing deformation researches used rigidity and excluded the shear strength parameters. On the other hand, the undrained shear strength parameter was deemed in the bearing capacity investigations for shallow foundations on clay, and the deformation behavior was excluded [25–27]. The current investigation defines soil strength and stiffness parameters as random fields for the reliability evaluation of strip footings on clay utilizing RFEM. The finite element analysis in the study considered the elasto-plastic clay-like soil behavior, deformation modulus and shear strength parameters (c and ϕ) were employed as random field inputs. The present work aims to create a sequence of hazard curves against maximum settlement and angular rotation for probabilistic shallow foundation design on clays. The current literature contains a related study on hazard curves for bearing capacity with the Tresca failure criterion [28]. However, the study covered ULS solution with a single shear strength parameter, and there was no previous study on hazard curves against footing deformations. The key contribution of the latter study is to develop a design framework for the reliability assessment of shallow foundations on spatially varying clay obeying the deformation limits in design codes. The proposed procedure will offer a valid method for RBD footings with SLS and probabilistic evaluation of strip footings taking soil spatial variability into account.

2. RANDOM FIELD FINITE ELEMENT METHOD (RFEM)

The controlling parameters of strip footing deformations on cohesive soils are the deformation modulus of soil E_d and the shear strength parameters c and ϕ. Defining these random field inputs is the initial step in developing the method. Once the random variable fits a probability distribution, the field is then determined by the correlation function, which depends on the variation distance of the random parameter in the field called correlation length θ. Markov correlation function in Eq.1 was adopted for 2D Gaussian random field case [7]:

$$\rho(\tau) = \exp\left(-\frac{|\tau|}{\theta_h} - \frac{|\tau|}{\theta_v}\right) \quad (1)$$

where τ is the distance between two random variables in the field, θ_h and θ_v are the horizontal and vertical correlation lengths, respectively.

2.1. Random Field Discretization and Meshing

The discretization of RF facilitated the assignment of a random variable in a random field mesh element. The continuous Gaussian random field function $f(\mathbf{x})$ became a set of $\hat{f}(x) = \{f_i\}$ by discretization. Non-Gaussian random variables were transformed into an equivalent Gaussian field since the discretization of the field employed linear transformation, which remained Gaussian after the process. In the latter research, the series expansion technique (SE) was employed for the random field discretization. The early studies on SE method

discretized the random field by spectral decomposition of Karhunen-Loeve (KL) series expansion [29,30]. The random field is represented as infinite series with standard normal variate ζ_i, eigenvalues λ_i, and eigenfunctions $g_i(\mathbf{x})$ of the correlation structure given in Eq.2:

$$f(\mathbf{x}) = \mu(\mathbf{x}) + \sigma \sum_{i=1}^{\infty} \xi_i \sqrt{\lambda_i} g_i(\mathbf{x}) \tag{2}$$

The eigenvalue problem is calculated using the integral solution of Eq.3:

$$\int_{\Omega} \rho(\mathbf{x},\mathbf{x}') g_i(\mathbf{x}') d\mathbf{x}' = \lambda_i g_i(\mathbf{x}) \tag{3}$$

In this way, a finite random variable of ζ_i represents the random field, and the discretized form of the field function with the r term is given in Eq.4. The truncation is applied with minor errors once the decay of the eigenvalues of expansion is described [31]. The truncation error was negligible since the terms having the highest eigenvalue were used.

$$\hat{f}(\mathbf{x}) = \mu(\mathbf{x}) + \sigma(\mathbf{x}) \sum_{i=1}^{r} \xi_i \sqrt{\lambda_i} g_i(\mathbf{x}) \tag{4}$$

There were developments in the approximation to the integral solution of the eigenvalue problem instead of directly solving Eq.3. One of the studies transformed the integral problem into a matrix eigenvalue problem by discrete integration rule [32]. Other approaches for the solution of Eq.3, such as Galerkin-type approximation [33] and wavelet-Galerkin scheme [34]. The present study discretized the random field by KL series expansion, and the eigenvalue problem was solved in MATLAB by transforming Eq.3 into a matrix form.

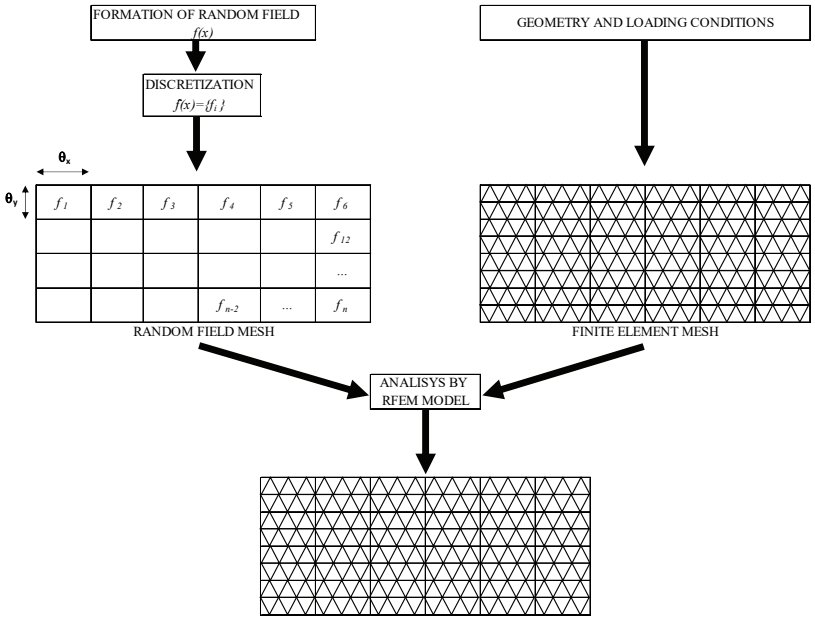

Fig. 1 - RFEM Meshing steps

Two separate meshes were recommended in the random field-based FEM analyses [35]. Theoretically, FEM and random field meshes are independent since their size selection criteria differ. FEM mesh size is selected by considering the model loading conditions and geometry. However, the random field mesh depends on the correlation length of the random parameter, and the random field mesh is more significant than the FEM mesh in RFEM. Fig. 1 illustrates the use of two meshes in RFEM solutions.

The current investigation followed the practical rule found in the literature. The random field mesh sizes are coarser than the FEM mesh sizes after the geometry, loading, and correlation length conditions are fulfilled [36]. The ratio of the random field mesh sizes to the varying correlation lengths was set to 1.

3. RFEM MODELLING OF SHALLOW STRIP FOOTING

The probabilistic results of the RFEM model for strip footing subjected to a vertical line load were investigated. The line load was determined as P=250kN/m, corresponding to the SLS characteristic settlement limit of 25 mm. Analyses were performed in finite element software ANSYS 2021 R2, and all the formulations of FEM and material models were taken from the theory reference of the code [37]. The overall equilibrium for the elastic static structural analysis is as follows:

$$[\mathrm{K}]\{u\} = \{F\} \tag{5}$$

where [K] is the total stiffness matrix (which is the sum of element stiffness matrices [K_e] over the N number of finite elements), {u} is the nodal displacement vector, and {F} is the load vector in Eq.5. The random field of (E_d) generated the probabilistic [K] matrix, which consists of the field realizations. The total stiffness matrix was then re-defined in the form of Eq.6 since the random field was defined by KL series expansion with r term and mean values of stiffness matrix [K_0]:

$$[K] = [K_0] + \sum_{i=1}^{r} [K_i]\xi_i \tag{6}$$

In that way, a probabilistic displacement vector {u} was obtained in RFEM. The influence of cohesive soil behavior was considered (models entitled CLAY henceforth), and the linear elastic-perfectly plastic Mohr-Coulomb model was employed so that c and ϕ constitute the yield surface. Since the shear strength parameters were random fields in the latter study, the stress vector {σ} in the fundamental stress-strain equation (Eq.7) also became probabilistic:

$$\{\sigma\} = [\mathrm{D}]\{\varepsilon^{el}\} = [D]\{\varepsilon - \varepsilon^{pl}\} \tag{7}$$

where [D] is the elasticity matrix, ε, ε^{el} and ε^{pl} are total, elastic, and plastic strain vectors, respectively. A representative model is demonstrated in Fig. 2; the drained condition of the soil was considered, and the groundwater level was assumed to be below the investigation depth of the soil layer. Soil and footing bodies were modeled using a 3D 10-Node tetrahedral structural solid (SOLID187). Concrete material properties were assigned to the footing solid.

Contact surfaces were defined between the footing and soil bodies: 3D 8-node surface-to-surface contact element (CONTA174) was associated with a 3D target segment (TARGE170) using shared geometric characteristics as the underlying element. The software allows the stiffness variation at the contact point as if there were springs with different stiffness values than the contact body stiffness at these points. The input of stiffness ratio is called FKN in the code, and the value of 0.67 was adopted by remaining within the typical interval of rigidity and strength ratio for soil-structure contacts [38].

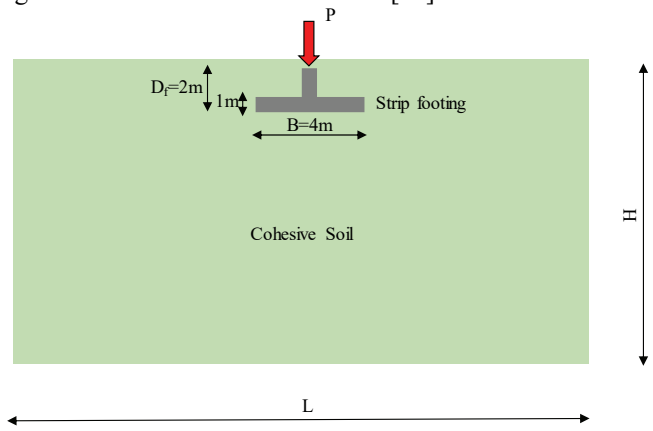

Fig. 2 - RFEM model of strip footing

3.1. Dimensions and Boundary Conditions

Dimensions of the soil body were formed so that the deformation contours were not affected by the boundaries (Fig. 3). RFEM model was created using 3D solid elements with 1-meter thickness, and the boundary restraints provided the plane strain conditions. The model base was fixed, deformations in the x and z axes were constrained on the sides, and the z-axis was constrained on the front and back. Model limits (H and L), dimensions of strip footing (B, t, D_f), loads (P), and physical properties of soil are kept deterministic. Poisson's ratio (ν) of

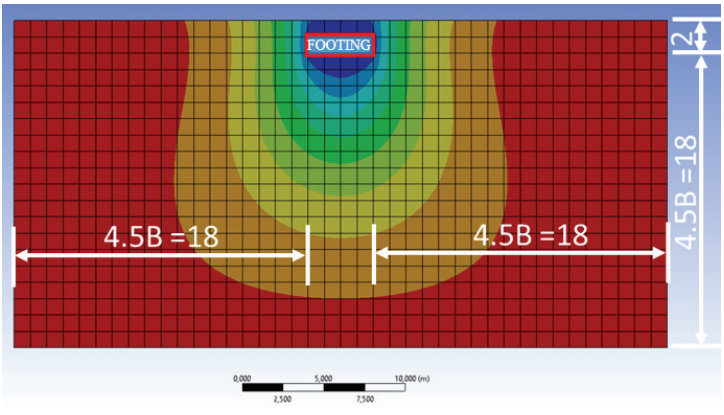

Fig. 3 - RFEM Model dimensions

soil was constant as a typical value of 0.35 for cohesive soils since the influence of ν variation in RFEM can be negligible [39].

3.2. Random Variables and Deformation Limits

Mean values of spatially varying inputs were selected as typical values in the literature [38,40]. The values are presented in three variability categories according to the coefficient of variations (COV): LOW, MID, and HIGH (Table 1).

Table 1 - Random variables in the model

Mean Values (μ)			
μ_E=15 MPa	**$\mu_{c'}$=5 kPa**	**$\mu_{\phi'}$=20°**	**Variability**
COV=0.60 (2-83 MPa)	COV=0.30 (2-13 kPa)	COV=0.10 (14-28°)	LOW
COV=0.70 (2-103 MPa)	COV=0.40 (1-17 kPa)	COV=0.15 (12-33°)	MID
COV=0.80 (1-126 MPa)	COV=0.50 (1-22 kPa)	COV=0.20 (10-38°)	HIGH

All the parameter limits remained within the ranges suggested in practice. Correlation lengths are given dimensionless ratio (Θ_h) in the horizontal direction in terms of B and the vertical-to-horizontal ratio in the vertical direction. The accepted values are given in Table 2, and the correlation length intervals remained within the limits recommended in the literature [41,42].

Table 2 - Correlation lengths in the analyses

Parameter	**Value**
$\Theta_h=\theta_h$ / B	0.25 0.50 1.00 2.50 5.00 10.00 (θ_h=1-40m)
θ_h / θ_v	2.00 10.00 (θ_v=0.1-20.0m)

Proposed hazard curves for maximum settlement and angular rotation of strip footing have been established according to the characteristic hazard limits found in the literature [43,44]: Safe Limit, Minor Damage, Medium Damage, and Major Damage (Table 3).

Table 3 - Deformation limits for hazard curves

Criteria		**Limit**
Total Max. Settlement (mm)	Safe Limit	25
	Medium Damage	35
	Major Damage	50
Angular Rotation (δ/B)	Minor Damage	1/1000
	Safe Limit	1/500
	Major Damage	1/250

3.3. Generation of RF Inputs

RF soil parameters were defined using an open-source MATLAB function called "randomfield" [45]. The function generates Gaussian random field realizations, given the RF mesh and correlation structure. RF inputs were assumed to fit a log-normal distribution to eliminate the negative values in the realizations. Mean (μ) and standard deviation (σ) were transformed into equivalent normal distribution forms to define Gaussian RF:

$$\sigma_{\ln} = \sqrt{\ln(1 + COV^2)} \qquad \mu_{\ln} = \ln(\mu) - 0.5\sigma_{\ln}^2 \tag{8}$$

RFEM models were constructed with the correlation lengths given in Table 2, and equivalent normal distribution parameters of each model were calculated using Eq.8 with the mean values and COVs. An exemplary process of RF realizations of the CLAY1 model for LOW variability has been elucidated. Standard Gaussian RF with μ=0 and σ=1 (g_i) was initially generated with the geometry and correlation info, and g_i was subsequently transformed into F_i field utilizing Eq.9:

$$F_i = \exp(\mu_{\ln} + \sigma_{\ln}.g_i) \tag{9}$$

Realizations of the E_d field were calculated as follows: $F_i = \exp(2.5543 + 0.5545.g_i)$. The process was iterated for RFs of shear strength inputs c and ϕ such that each RFEM model contained nine random fields for three main inputs and three variability categories. Representative realizations of each parameter for CLAY1 model LOW variability were given in Fig. 4. The parameter fluctuations along depth and in the horizontal direction depicted the intrinsic soil uncertainty owing to geological conditions such as stratification, faulting, soil deposition, over-consolidation, or desiccation.

3.4. Analysis Framework

The RFEM analysis algorithm in the study started by generating RFs for soil stiffness and shear strength parameters using MATLAB. The function automatically discretized RFs by the KL series expansion method. CLAY models were established in FEM software, and the soil body was divided into tiny rectangular prisms according to the values of θ_h and θ_v. Each value in the RF realizations of the inputs was assigned to the center of the corresponding random field mesh elements. The overall model geometry is listed in Fig. 5. Each model contained c ϕ and E_d RFs simultaneously, and RFEM models were set to analyze one thousand iterations involving all realizations with three variability categories. Thus, each model performed three thousand iterations for all variabilities. The histograms of footing deformations were attained, whereupon the analyses and appropriate probability density functions (PDF) were fitted to the output distributions. PDFs were utilized to estimate the P_fs for the deformation limits. The values of P_f, θ_h and θ_v constructed the proposed hazard curves, and each hazard curve comprised three damage limits for RBD of a shallow foundation according to multiple damage limits. The main framework of the investigation explained is illustrated in Fig. 6.

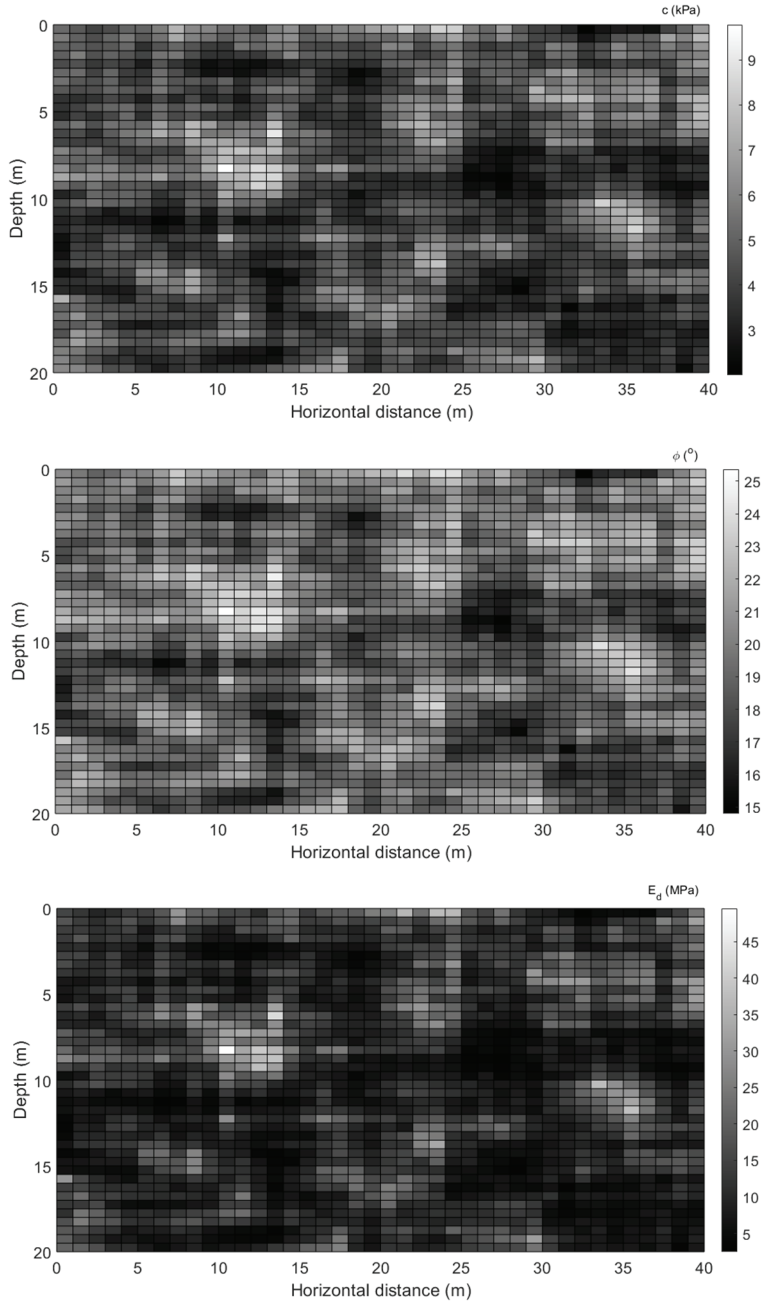

Fig. 4 - Representative realizations of c, ϕ, E_d RFs for CLAY1 model LOW variability category

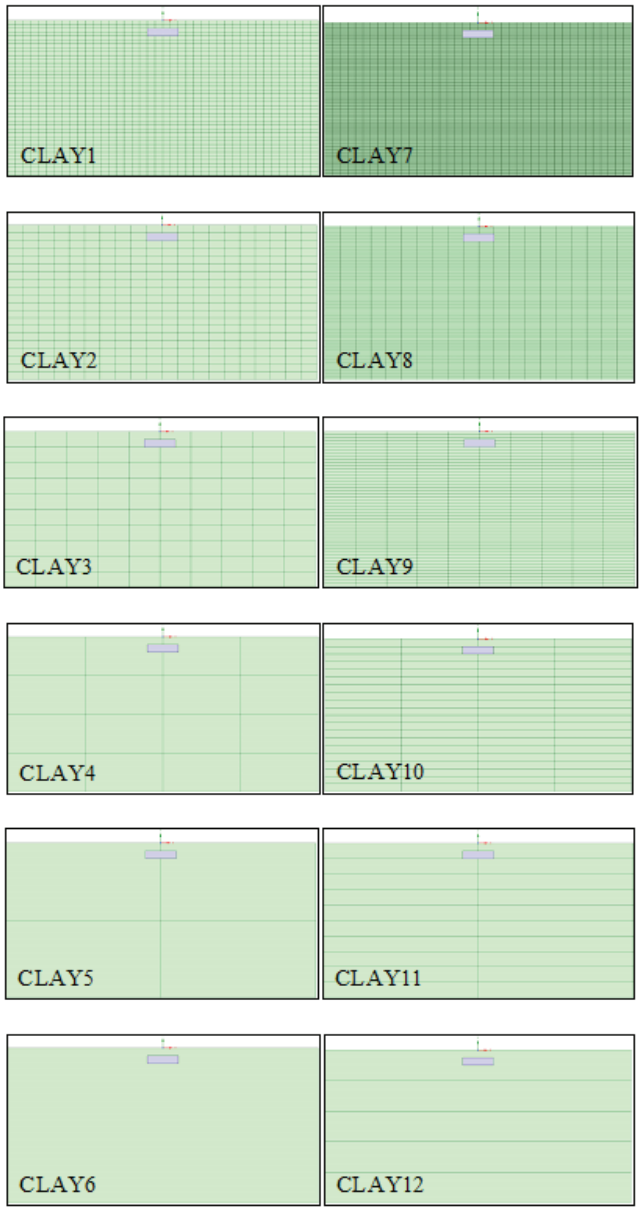

Fig. 5 - RFEM models in ANSYS

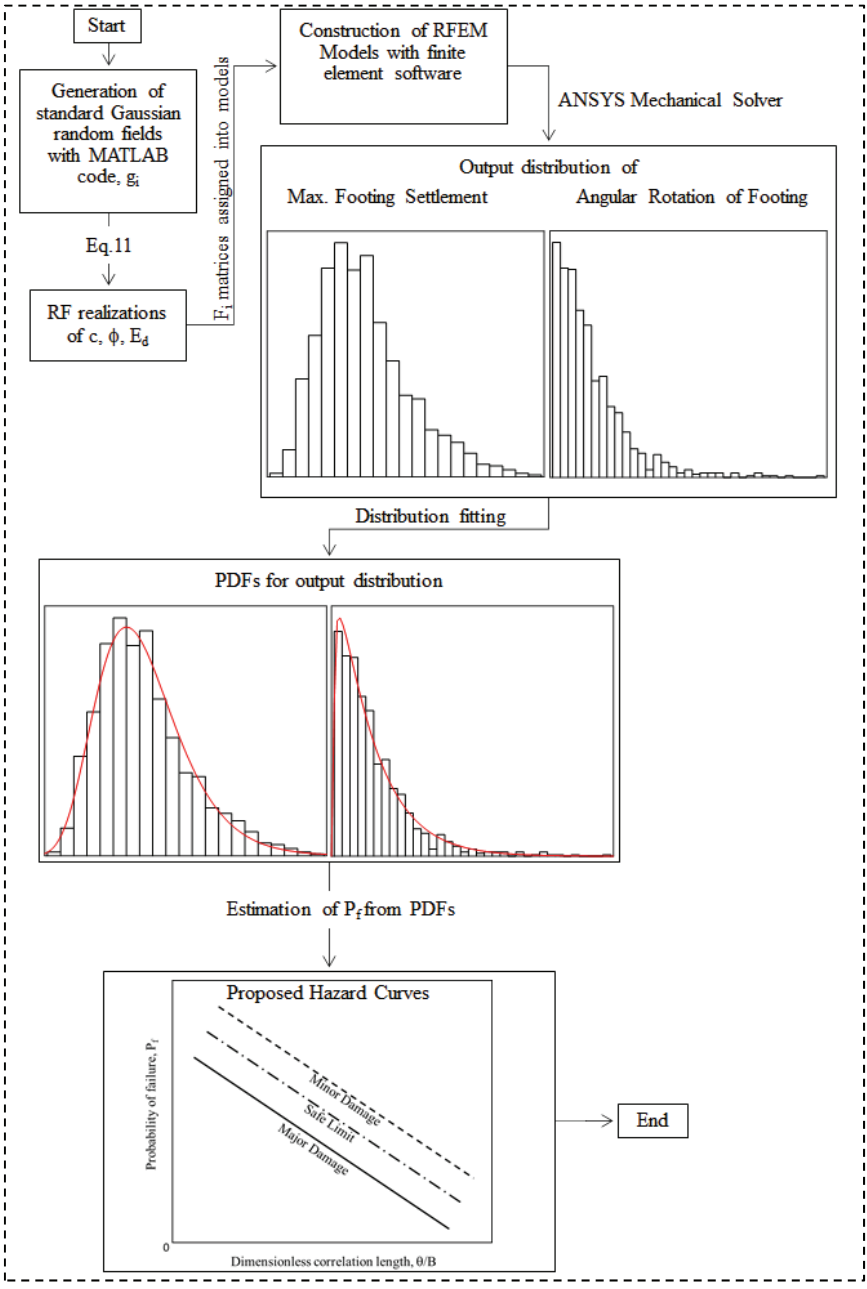

Fig. 6 - Main algorithm for the development of the proposed hazard curves

4. RESULTS

Vertical nodal displacements on the left and right edges of the footing (u_{left}, u_{rigth}) were recorded. The absolute maximum of these nodal displacements represented the total settlement (s_{max}), and the absolute difference between them represented the angular rotation ($\tan\alpha$) depicted in Fig. 7.

Each model performed the iterations, and six output distributions were obtained for all variability categories (three for total settlement and three for angular rotation). Log-normal PDF fitted the total settlement outputs (Fig. 8a), and Gamma distribution fitted the angular rotation results (Fig. 8b).

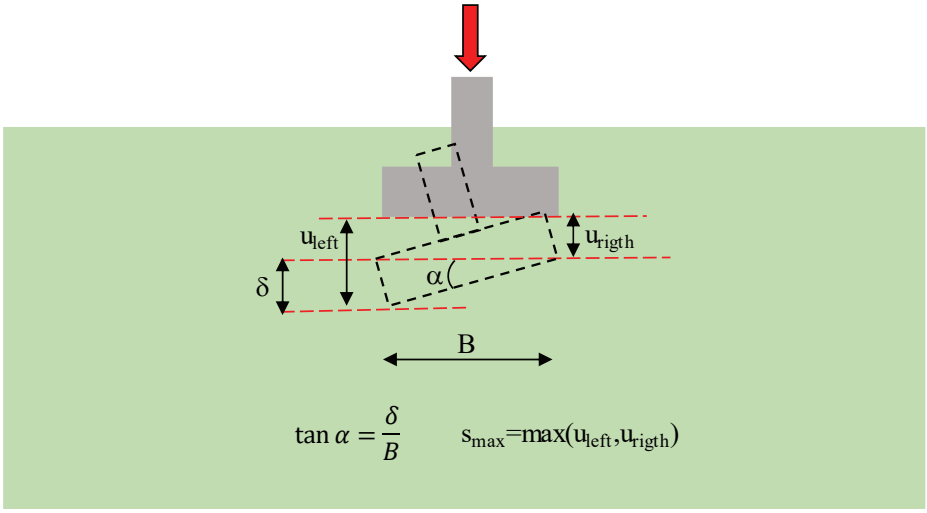

Fig. 7 - Maximum total settlement and angular rotation of the strip footing

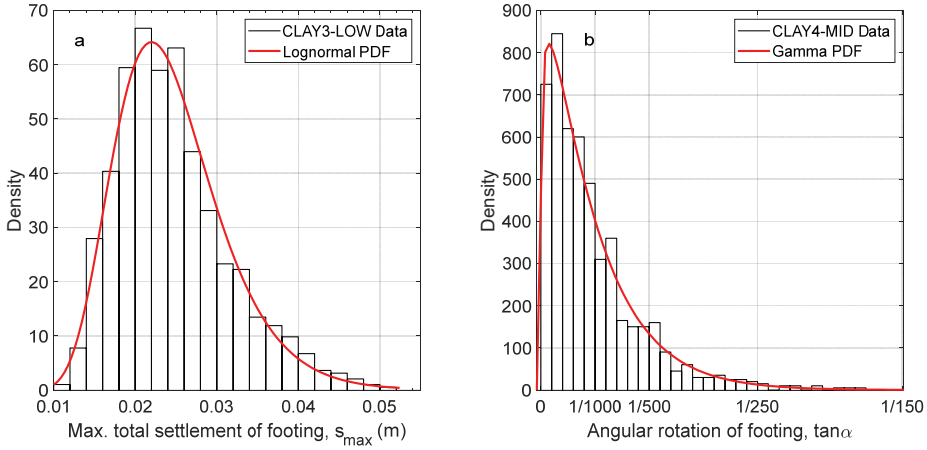

Fig. 8 - Representative PDFs for max. total settlement (a), and angular rotation (b) outputs

4.1. Hazard Curves for Total Maximum Settlement of Strip Footing

The distribution fitter tool was utilized to derive the log-normal cumulative distribution function (CDF) of output PDFs allowing P_f to be estimated directly. All values were reported within a 95% confidence interval, and a sample CDF was presented in Fig. 9. The multiple θ_h/θ_v ratios allowed the anisotropic soil behavior to be considered along with three variability categories. Fig. 10 depicts six proposed total settlement hazard curves for the variability and anisotropy categories. Each color in the graphs embodies different hazard limits, and dashed lines are the confidence bounds of the corresponding hazard curve. Hazard curves illustrated minor deviations in failure probabilities beyond Θ_h=1.0~2.5 relative to changes up to this critical interval. Since the larger the soil volume under the foundation up to a critical value in footing size, the greater the impact of the soil spatial variation.

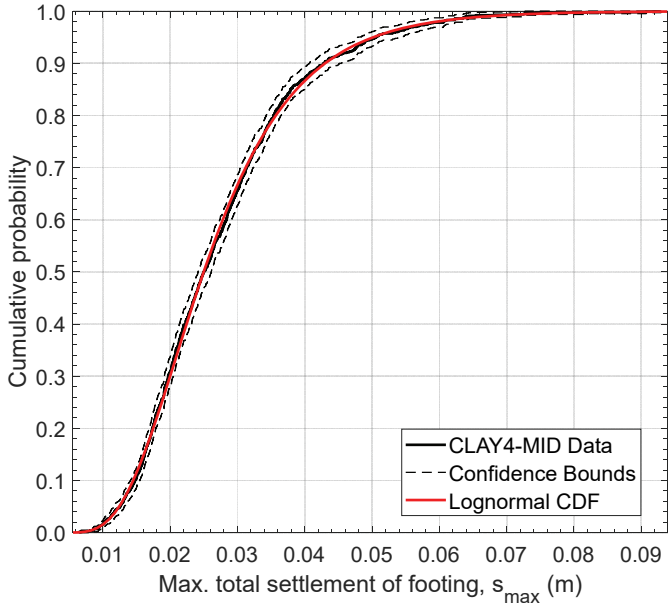

Fig. 9 - Representative CDF for total settlement

4.2. Hazard Curves for Angular Rotation of Strip Footing

The analogy explained in section 4.1 was followed, and Gamma CDF outputs with the 95% confidence level were constructed. The horizontal axis in the CDF plot has been given in fractions obeying the common notation of rotational limits in practice (Fig. 11). Proposed six hazard curves for angular rotation of strip footing was given in Fig. 12.

All the angular rotation plots showed a peak at Θ_h=5, and beyond this value the curves dropped off dramatically near zero, meaning there was no angular rotation in the foundation. In other words, the impact of soil spatial variation in the horizontal direction was critical up

to five times the footing size. Beyond this limit, the soil layer below the footing behaved uniformly regarding soil variability, and no angular rotation occurred.

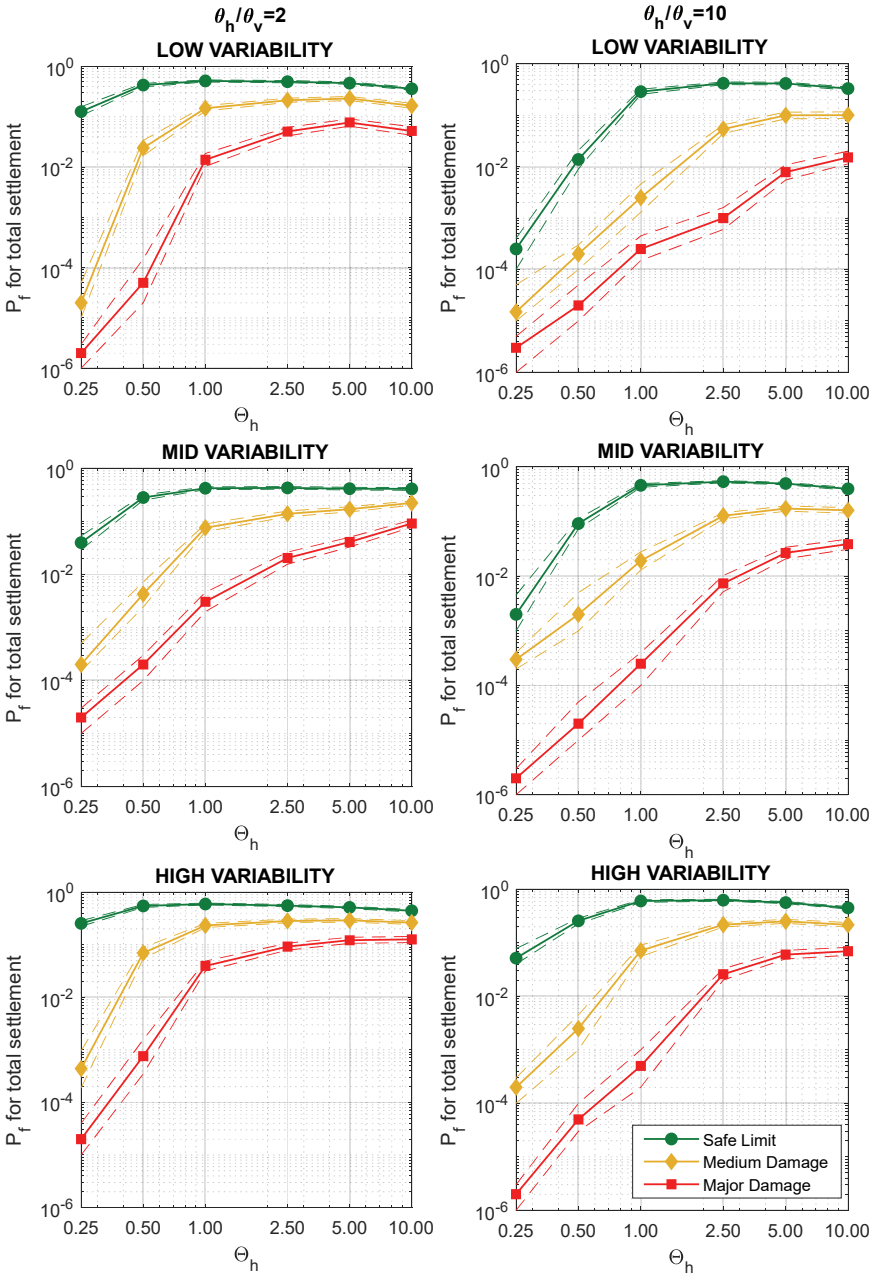

Fig. 10 - Proposed hazard curves for maximum total settlement of strip footing

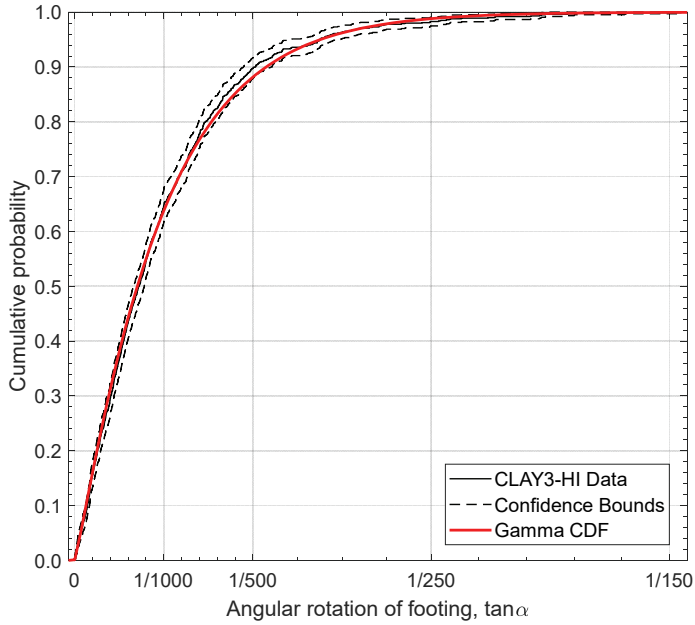

Fig. 11 - Representative CDF for angular rotation output

4.3. Verifications

The effect of mesh scenarios on the deformation behavior of the shallow footing model was examined. Triangular meshes were first generated on a test model with uniform element size, and the settlement of the foundation for this case was recorded. Refined mesh around the footing body was then applied, and the results of this case were also recorded. Load-deformation curves for refined and uniform meshes were compared, and it was confirmed that changing the mesh settings did not influence the deformation behavior.

The RF generation method in the present study was adapted to a reference study on RFEM evaluation of shallow footing. The reference model contained a random field of elasticity modulus for soil [20]. Fig. 13 demonstrates a representative realization of E from the reference work with a mean and standard deviation of 40 MPa and uniform RF with θ=3m.

RF from the prior study was re-generated utilizing the technique of the current research with relatively close ranges to the verification reference. Two representative realizations were given, confirming the validation of the RF generation method used (Fig. 14).

The RF generation function automatically truncated the KL expansion, eliminating the need for a truncation error estimate. For instance, 1600 eigenvalues were employed to generate the 40x40 RF model. The decay of eigenvalues of a representative RF generation demonstrated that the function efficiently truncates the expansion (Fig. 15). All RF generations were controlled utilizing the decay of eigenvalues and the decline was shown to converge to zero, confirming the slight truncation error [31].

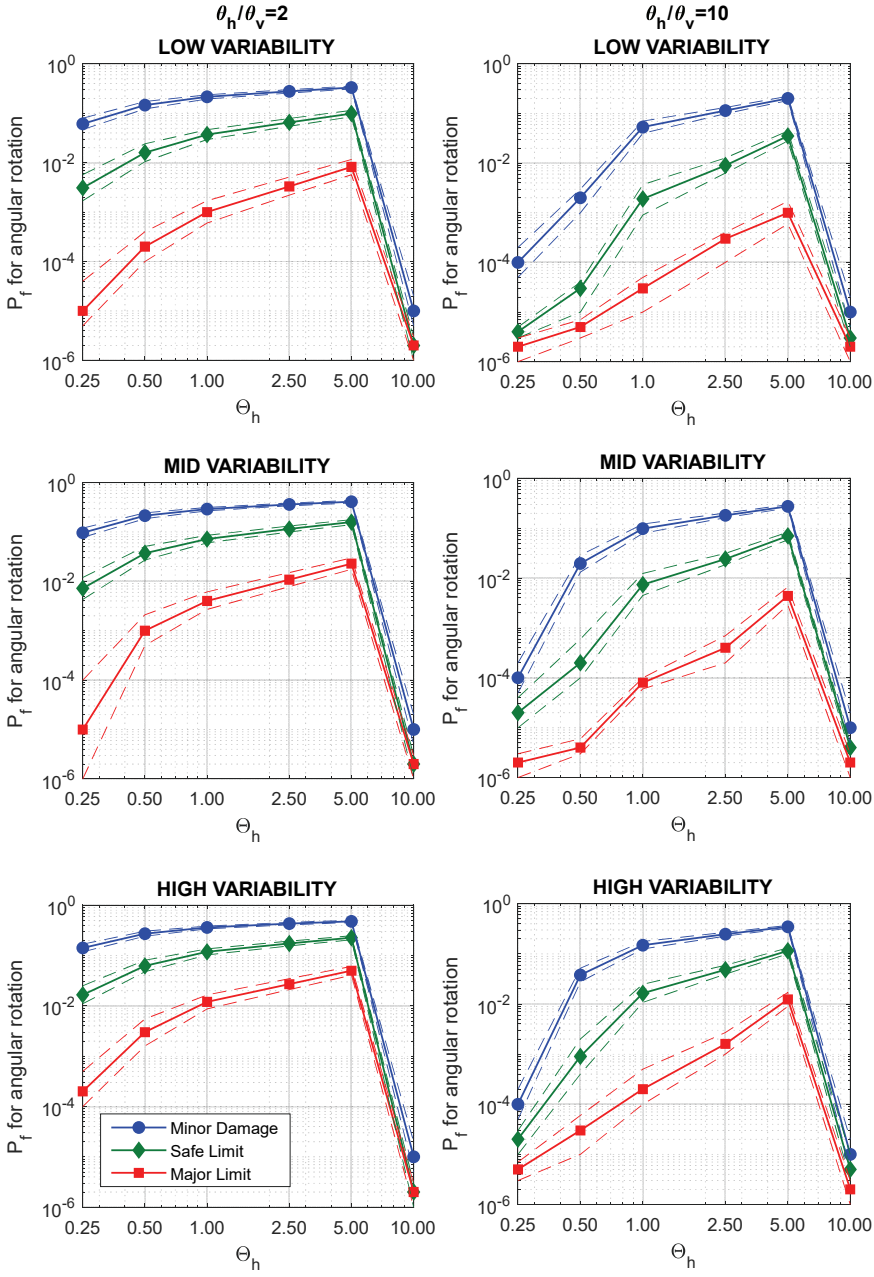

Fig. 12 - Proposed hazard curves for absolute angular rotation of strip footing

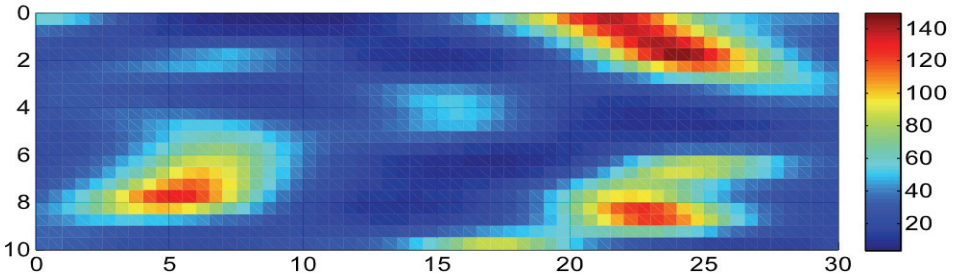

Fig. 13 - Representative realization from verification reference [20]

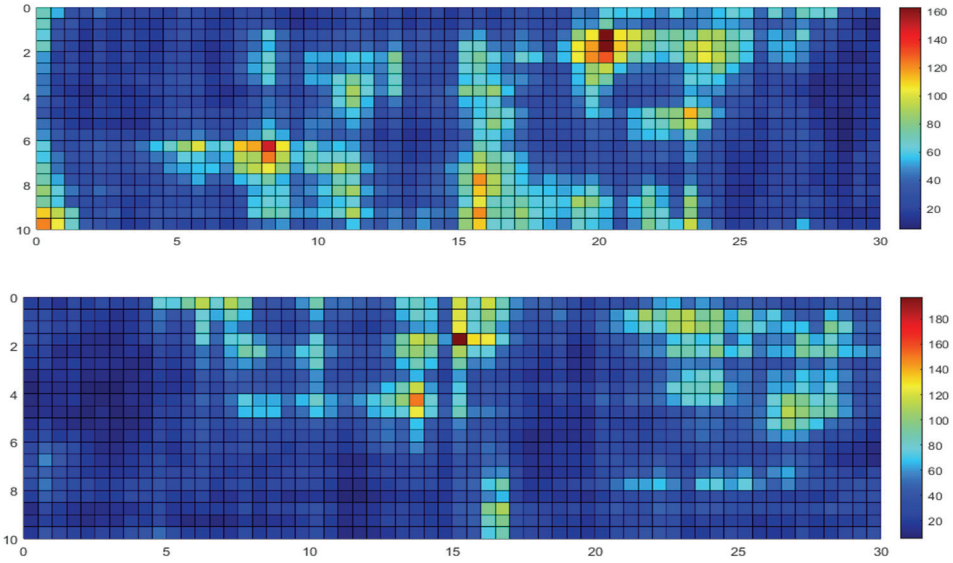

Fig. 14 - Realizations by the method in the present work with the parameters of reference study

The verification reference was also used for the analysis steps confirmation of the current investigation. RFEM attained the total footing settlement with five thousand realizations according to the reference model. Fig. 16 delineates the comparison of reference and calculated output PDFs, and it was found that the outputs of the method were close to the findings of the reference study. Thus, the main framework in the present study has been verified.

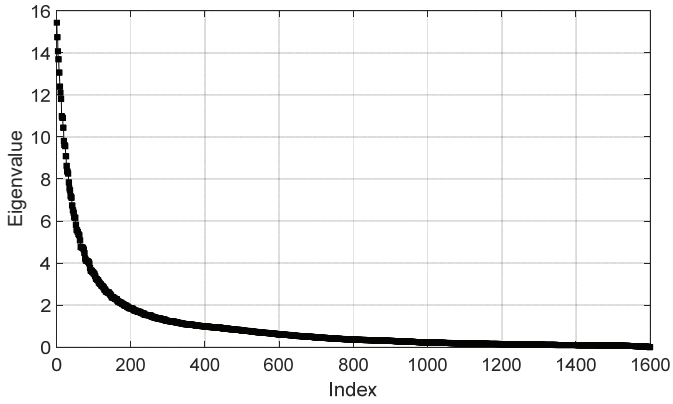

Fig. 15 - The decay in eigenvalue for a representative RF generation

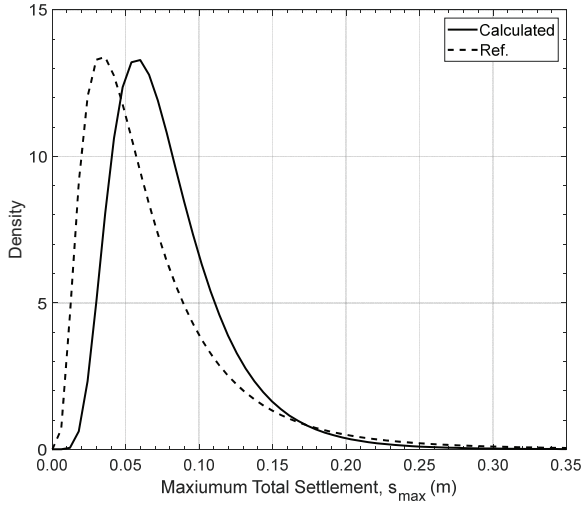

Fig. 16 - Output PDFs calculated by the present method and adopted from the reference study

4.4. Validation of Proposed Hazard Curves

Proposed hazard curves enable the evaluation of shallow foundations utilizing RBD criteria following the soil horizontal and vertical spatial variation in a studied region. Since this type of guidance must be validated before use, a calibration model was produced in the current work analogous to the RFEM models. An actual database was employed to generate RF inputs of the validation model, and the outputs were compared with the proposed hazard curves. An open-source CPT database (304dB) from the International Society of Soil Mechanics and Geotechnical Engineering (ISSMGE) Technical Committee for Risk

Assessment TC304 was used in the validation study. The database entitled TX-CPTU was used to evaluate the proposed hazard curves. The corresponding database contains 9 CPT soundings on stiff over-consolidated CL/CH clays from a region in Baytown, TX, USA. The horizontal spacing of each test point varies between 7.6 to 28.7 m, and the testing depths vary between 3.7 to 15.3m. Extensive research in the region reported that the mean value of correlation length was 0.849m in the vertical direction and 5.830m in the horizontal direction [46]. Thus, θ_v=0.800m and θ_h=5.800m were assumed in the RFEM validation model. The statistical values of RF inputs (E_d, c, and ϕ) were calculated by CPT correlations [47–49], and RFs were generated from 9 CPT in the database. Statistical information of the validation model was summarized in Table 4, and the low variability category was set for the region according to the input COVs.

Table 4 - RF input statistics from the TX-CPTU database

Parameter		**Average**	**Minimum**	**Maximum**
E_d (kPa)	μ	47089	39480	57560
	σ	13967	10260	16607
	COV (%)	29.8	24.1	39.3
c' (kPa)	μ	5.0	3.6	5.8
	σ	4.2	2.8	7.0
	COV (%)	84.2	60.4	131.2
ϕ' (°)	μ	35.8	32.4	38.2
	σ	5.5	4.1	7.0
	COV (%)	15.4	12.4	18.2

The validation model was iteratively solved in FEM code for one thousand realizations, and outputs of total settlement and angular rotation of the strip footing were recorded. Failure probabilities were consequently estimated for the results using the hazard limits. According to the correlation lengths of the validation database, θ_h/B=5.8/4= 1.45 and θ_h/θ_v=5.8/0.8= 7.25 were found. Therefore, the comparison was performed employing the low variability hazard curve with θ_h/θ_v=10 for total settlement and angular rotation. The results were scattered on the corresponding hazard curves, and all resulting points were within the confidence bounds of the curves confirming that the use of proposed hazard curves is valid for RBD of shallow footings on cohesive soils (Fig. 17).

4.5. Worked Example

Many international regulations include the reliability-based design of shallow foundations; for example, ISO has published a standard for the reliability of structures that accepts the probabilistic methods to achieve target reliability [5]. The standard accepts first-order reliability methods (FORM) or full probabilistic methods such as RFEM. Implementation of

the proposed procedure in this context is demonstrated using a worked example of a steel-framed industrial structure supported by 3m wide strip footings sitting on cohesive soil at 1.5m depth. The geometrical detail of the example structure is illustrated in Fig. 18.

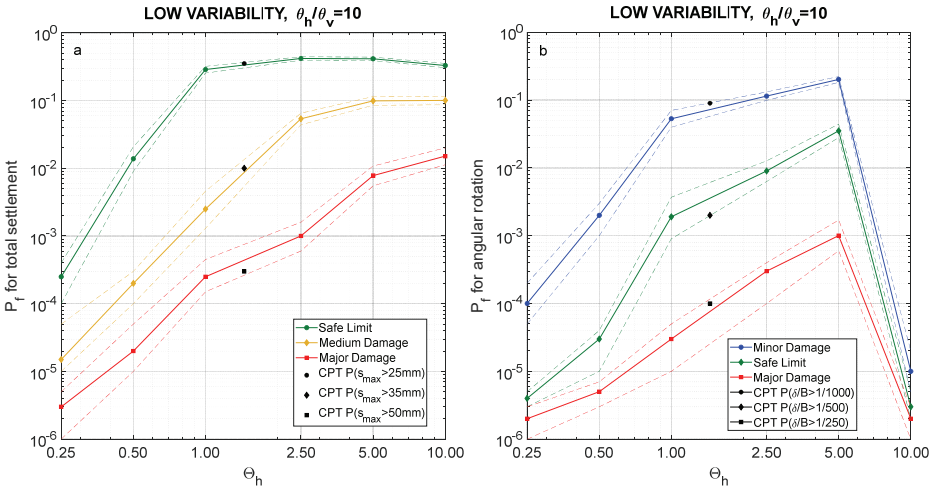

Fig. 17 - Validation of hazard curves with CPT database

A vertical load combination was applied, and the imposed loads for a typical industrial structure were adopted. The exemplary combination of dead load (DL) and live load (LL) was assumed as follows: DD+LL=5+7.5 kN/m2. The results of one frame were considered, and the calculations were given per frame (plane strain condition). It was presumed that a sufficient quantity of soil samples had been collected for the reliability assessment. Soil properties were taken as the mean values from Table 2; μ_E =15MPa, $\mu_{c'}$=5kPa, μ_ϕ=20°, and COVs 0.70, 0.40, 0.15, respectively; confirming the medium variability condition. In addition, soil spatial variability evaluation was assumed to be performed, and θ_h =3.00m θ_v=1.50m was given.

The requirement was to check the existing footing dimensions for the listed parameters. The intermediate structural tolerance to footing settlement was assumed to take the medium damage limits into account. Initially, the analytical (so-called deterministic) solution for SLS calculated the minimum required footing width. Consequently, the soil variation was considered, and computations were performed for the target reliability index (β_{Target}). ISO-2394:2051, in cooperation with JCSS (Joint Committee of Structural Safety), recommends a target reliability index (with associated failure probability) for a one-year reference period with irreversible SLS of β=1.70($P_f \approx 5.10^{-2}$)[50]. The hazard curve for θ_h/θ_v=3.00/1.50=2.00 and MID variability category was selected, and P_f was read for $\Theta_h=\theta_h/B$=3/3=1 as 8.10^{-2} (β=1.40<β_{Target}). Since the target reliability was not fulfilled, the footing dimension should be adjusted accordingly. From the corresponding hazard curve, $\Theta_h \approx 0.90$ was read off for the corresponding target $P_f=5.10^{-2}$. Thus, the resized footing dimension was as follows: $\Theta_h=\theta_h/B$,

0.90=3.00/B => B=3.33m. FORM also computed the footing dimension for β_{Target}, and the summary results of comparison with the proposed method are listed in
Table *5*. The comparison disclosed that the prior footing size was insufficient. Furthermore, it was also noted that the analytic solution does not meet the reliability assessment requirements. Therefore, the aid of a probabilistic technique was essential, particularly in the case of high fluctuation in soil properties.

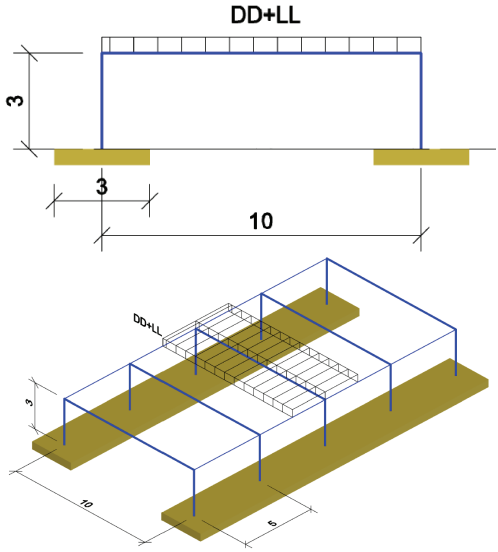

Fig. 18 - Structural geometry of the worked example

Table 5 - Comparison of footing dimensioning by different methods

		Analytical	**Probabilistic Methods**	
	Given	Required by SLS	FORM	Proposed Hazard Curves
Footing Dimension, B (m)	3.00	3.15	3.36	3.33

FORM and the proposed method gave analogous results, but the technique only considered variation in soil properties, not spatial variability. On the other hand, the proposed framework highlighted the necessity of evaluating the spatial variability for RBD of the strip footings by SLS. Table 6 exhibits the differentiation of FORM and the presented method results for footing sizes when considering the spatial variation of soil. The results of the proposed hazard curves indicated that if spatial variability is overlooked in a reliability assessment, the dimensioning could be over- or under-designed depending on the rate of ground uncertainty. The proposed procedure of the latter research has efficiently described this case.

Table 6 - Comparison of dimensioning results for different spatial variability cases

θ_h (m)	θ_v (m)	B_{FORM} (m)	β from hazard curves	$B_{Proposed}$ (m) for β_{Target}=1.70
3.00	1.50	3.36	1.40	3.33
10.00	1.00	3.36	1.00	5.00

5. CONCLUSION

The present work proposed hazard curves for footing deformation of strip foundations on cohesive soils with the variability and anisotropy categories. Hazard curves were constructed considering the variations in soil shear strength and rigidity parameters. The multiple θ_h/θ_v ratios allowed the anisotropic soil behavior to be considered along with three variability categories The necessity of quantifying soil spatial variability for RBD of strip footings on cohesive soils was underlined.

Overall settlement hazard curves exhibited minor deviation in failure probabilities over Θ_h=1.0~2.5 compared to variations up to this critical range. The reason was that the larger the soil volume under the foundation up to a decisive value in size B, the greater the impact of the soil spatial variation.

All plots for angular rotation showed a peak at Θ_h=5, and beyond this value curves dropped off dramatically near zero, meaning there was no angular rotation in the footing. In other words, the influence of spatial variation of soil in the horizontal direction was critical up to five times the footing size. Beyond this limit, the soil layer below the foundation behaved uniformly regarding soil variability, and no angular rotation occurred.

Proposed hazard curves for shallow foundations were introduced to the literature, considering both elasto-plastic soil behavior with the Mohr-Coulomb failure criterion and the impact of all influencing parameters that comply with the deformation limits in the foundation regulations. The proposed technique provided a probabilistic study of strip foundations considering the spatial variation of clayey soils and a valid procedure for RBD with SLS.

Declaration of Competing Interest

The authors declare that they have no known competing financial interests or personal relationships that could have appeared to influence the work reported in this paper.

Acknowledgments

The authors would like to thank the members of the TC304 Committee on Engineering Practice of Risk Assessment & Management of the ISSMGE for developing the database 304dB used in this study and making it available for scientific inquiry. We also wish to thank Armin D. Stuedlein for contributing this database to the TC304 compendium of databases. A part of the study was conducted under the support of the scientific research project within the doctoral study of the corresponding author at Istanbul Kultur University (Grant No: BAP2202).

Abbreviations

CDF	: cumulative distribution function
COV	: coefficient of variation
CPT	: cone penetration test
DD	: dead load
FE	: finite elements
FEM	: finite element method
FKN	: normal stiffness factor
FORM	: first order reliability method
KL	: Karhunen-Loeve
LL	: live load
MC	: Mohr-Coulomb
PDF	: probability density function
RBD	: reliability-based design
RF	: random field
RFEM	: random finite element method
SFEM	: stochastic finite element method
SLS	: serviceability limit state

Symbols

α	: rotation angle
β	: reliablity index
δ	: settlement difference
ε, ε^e, ε^p	: total, elastic and plastic strain
ϕ	: angle of shearing resistance
λ_i	: eigenvalue of random field
μ	: mean
ν	: Poisson's ratio
Ω	: random field domain
ρ	: correlation function

σ : standard deviation

$\{\sigma\}$: stress vector

θ, θ_h, θ_v : correlation length, horizontal and vertical correlation length

Θ_h : dimensionless horizontal correlation length

τ : distance between two random variables

$\xi_i(\theta)$: standard normal variate

B : footing width

c : soil cohesion

D : elasticity matrix

D_f : depth of embedment

E, E_d : modulus of elasticity, deformation modulus of soil

{F} : load vector

F_i : random field matrix

f_i : random field realization

$g_i(\mathbf{x})$: eigenfunction of random field

[K] : rigidity matix

P_f : probability of failure

s_{max} : maximum total settlement

t : footing thickness

{u} : displacement vector

x : random variable vector

x_i : random variable

References

[1] EN-1997-1, Eurocode 7: Geotechnical design- Part 1: General Rules, CEN European Committee for Standardization, Brussels, 2004.

[2] K.K. Phoon, F.H. Kulhawy, Characterization of geotechnical variability, Can. Geotech. J. 36 (1999) 612–624. https://doi.org/10.1139/t99-038.

[3] K.K. Phoon, F.H. Kulhawy, Evaluation of geotechnical property variability, Can. Geotech. J. 36 (1999) 625–639. https://doi.org/10.1139/t99-039.

[4] EN-1990:2002, Eurocode. Basis of Structural Design, CEN European Committee for Standardization, Brussels, 2002.

[5] ISO-2394:2015, General Principles on Reliability of Structures., International Organization for Standardization, Geneva, 2015.

[6] E.H. Vanmarcke, Probabilistic Modeling of Soil Profiles, ASCE J Geotech Eng Div. 103 (1977) 1227–1246. https://doi.org/10.1016/0148-9062(78)90012-8.

[7] E.H. Vanmarcke, Random Fields: Analysis and Synthesis, World Scientific, London&New Jersey, 2010. https://doi.org/https://doi.org/10.1142/5807.

[8] G.B. Beacher, T.S. Ingra, Stochastic Fem in Settlement Predictions, J. Geotech. Eng. Div. 107 (1981) 449–463. https://doi.org/10.1061/ajgeb6.0001119.

[9] D. V. Griffiths, G.A. Fenton, Probabilistic settlement analysis by stochastic and random finite-element methods, J. Geotech. Geoenvironmental Eng. 135 (2009) 1629–1637. https://doi.org/10.1061/(ASCE)GT.1943-5606.0000126.

[10] A. Ahmed, A.H. Soubra, Probabilistic analysis of strip footings resting on a spatially random soil using subset simulation approach, Georisk. 6 (2012) 188–201. https://doi.org/10.1080/17499518.2012.678775.

[11] G.A. Fenton, D. V. Griffiths, Risk Assessment in Geotechnical Engineering, John Wiley & Sons, Inc., Hoboken, NJ, USA, 2008. https://doi.org/10.1002/9780470284704.

[12] G.M. Paice, D. V. Griffiths, G.A. Fenton, Finite element modeling of settlements on spatially random soil, J. Geotech. Eng. 122 (1996) 777–779. https://doi.org/10.1061/(asce)0733-9410(1996)122:9(777).

[13] A. Ahmed, A.H. Soubra, Probabilistic analysis at the serviceability limit state of two neighboring strip footings resting on a spatially random soil, Struct. Saf. 49 (2014) 2–9. https://doi.org/10.1016/j.strusafe.2013.08.001.

[14] G.A. Fenton, D. V. Griffiths, Three-dimensional probabilistic foundation settlement, J. Geotech. Geoenvironmental Eng. 131 (2005) 232–239. https://doi.org/10.1061/(ASCE)1090-0241(2005)131:2(232).

[15] T. Al-Bittar, A.H. Soubra, Probabilistic analysis of strip footings resting on spatially varying soils and subjected to vertical or inclined loads, J. Geotech. Geoenvironmental Eng. 140 (2014). https://doi.org/10.1061/(ASCE)GT.1943-5606.0001046.

[16] J.T. Simões, L.C. Neves, A.N. Antão, N.M.C. Guerra, Reliability assessment of shallow foundations on undrained soils considering soil spatial variability, Comput. Geotech. 119 (2020) 103369. https://doi.org/10.1016/j.compgeo.2019.103369.

[17] D. V. Griffiths, G.A. Fenton, Bearing capacity of spatially random soil: The undrained clay Prandtl problem revisited, Geotechnique. 51 (2001) 351–359. https://doi.org/10.1680/geot.2001.51.4.351.

[18] M.J. Cassidy, M. Uzielli, Y. Tian, Probabilistic combined loading failure envelopes of a strip footing on spatially variable soil, Comput. Geotech. 49 (2013) 191–205. https://doi.org/10.1016/j.compgeo.2012.10.008.

[19] J. Ching, Y.G. Hu, Effective Young's Modulus for a Footing on a Spatially Variable Soil Mass, Geotech. Spec. Publ. (2017) 360–369. https://doi.org/10.1061/9780784480717.034.

[20] Q. Yue, J. Yao, Soil deposit stochastic settlement simulation using an improved autocorrelation model, Probabilistic Eng. Mech. 59 (2020) 103038. https://doi.org/10.1016/j.probengmech.2020.103038.

[21] A.E. Kenarsari, R. Jamshidi Chenari, Probabilistic settlement analysis of shallow foundations on heterogeneous soil stratum with anisotropic correlation structure, Geotech. Spec. Publ. GSP 256 (2015) 1905–1914. https://doi.org/10.1061/9780784479087.174.

[22] A. Johari, A. Sabzi, A. Gholaminejad, Reliability Analysis of Differential Settlement of Strip Footings by Stochastic Response Surface Method, Iran. J. Sci. Technol. - Trans. Civ. Eng. 43 (2019) 37–48. https://doi.org/10.1007/s40996-018-0114-3.

[23] K. Winkelmann, K. Żyliński, A. Korzec, J. Górski, Effectiveness of Random Field Approach in Serviceability Limit State Analysis of Strip Foundation, Geotech. Geol. Eng. 40 (2022) 4705–4720. https://doi.org/10.1007/s10706-022-02179-6.

[24] E. Arel, A.C. Mert, Field simulation of settlement analysis for shallow foundation using cone penetration data, Probabilistic Eng. Mech. 66 (2021) 103169. https://doi.org/10.1016/j.probengmech.2021.103169.

[25] S.K. Jha, Reliability-based analysis of bearing capacity of strip footings considering anisotropic correlation of spatially varying undrained shear strength, Int. J. Geomech. 16 (2016) 1–10. https://doi.org/10.1061/(ASCE)GM.1943-5622.0000638.

[26] Y. Wu, X. Zhou, Y. Gao, S. Shu, Bearing capacity of embedded shallow foundations in spatially random soils with linearly increasing mean undrained shear strength, Comput. Geotech. 122 (2020) 103508. https://doi.org/10.1016/j.compgeo.2020.103508.

[27] C. Mendoza, J.E. Hurtado, The Importance of Geotechnical Random Variability in the Elastoplastic Stress–Strain Behavior of Shallow Foundations Considering the Geological History, Geotech. Geol. Eng. 40 (2022) 3799–3818. https://doi.org/10.1007/s10706-022-02132-7.

[28] R. Popescu, G. Deodatis, A. Nobahar, Effects of random heterogeneity of soil properties on bearing capacity, Probabilistic Eng. Mech. 20 (2005) 324–341. https://doi.org/10.1016/j.probengmech.2005.06.003.

[29] M.A. Lawrence, Basis random variables in finite element analysis, Int. J. Numer. Methods Eng. 24 (1987) 1849–1863. https://doi.org/10.1002/nme.1620241004.

[30] P.D. Spanos, R. Ghanem, Stochastic finite element expansion for random media, J. Eng. Mech. 115 (1989) 1035–1053. https://doi.org/10.1061/(ASCE)0733-9399(1989)115:5(1035).

[31] S.P. Huang, S.T. Quek, K.K. Phoon, Convergence study of the truncated Karhunen-Loeve expansion for simulation of stochastic processes, Int. J. Numer. Methods Eng. 52 (2001) 1029–1043. https://doi.org/10.1002/nme.255.

[32] D. Mirfendereski, On series representation of random fields and their application in stochastic finite element analysis, California, 1990.

[33] R.G. Ghanem, P.D. Spanos, Spectral stochastic finite-element formulation for reliability analysis, J. Eng. Mech. 117 (1991) 2351–2372. https://doi.org/10.1061/(ASCE)0733-9399(1991)117:10(2351).

[34] K.K. Phoon, S.P. Huang, S.T. Quek, Implementation of Karhunen-Loeve expansion for simulation using a wavelet-Galerkin scheme, Probabilistic Eng. Mech. 17 (2002) 293–303. https://doi.org/10.1016/S0266-8920(02)00013-9.

[35] A. Der Kiureghian, J. Bin Ke, The stochastic finite element method in structural reliability, Probabilistic Eng. Mech. 3 (1988) 83–91. https://doi.org/10.1016/0266-8920(88)90019-7.

[36] P.L. Liu, A. Der Kiureghian, Finite element reliability of geometrically nonlinear uncertain structures, J. Eng. Mech. 117 (1991) 1806–1825. https://doi.org/10.1061/(ASCE)0733-9399(1991)117:8(1806).

[37] P. Kohnke, Theory Reference for the Mechanical APDL and Mechanical Applications, Canonsburg, PA, 2009.

[38] J.E. Bowles, Foundation Analysis and Design, McGraw-Hill, 1997. https://books.google.com.tr/books?id=iuBwtgAACAAJ.

[39] G.A. Fenton, D. V. Griffiths, Probabilistic foundation settlement on spatially random soil, J. Geotech. Geoenvironmental Eng. 128 (2002) 381–390. https://doi.org/10.1061/(ASCE)1090-0241(2002)128:5(381).

[40] M. Budhu, Soil Mechanics and Foundations, 3rd Edition, John Wiley & Sons, Incorporated, 2010. https://books.google.com.tr/books?id=ga8bAAAAQBAJ.

[41] F.H. Kulhawy, K.K. Phoon, M. Grigoriu, E.P.R. Institute, C.U.G.E. Group, Reliability-based Design of Foundations for Transmission Line Structures, Prepared for Electric Power Research Institute, 1995. https://books.google.com.tr/books?id=dSpUAAAAYAAJ.

[42] M. Lloret-Cabot, G.A. Fenton, M.A. Hicks, On the estimation of scale of fluctuation in geostatistics, Georisk. 8 (2014) 129–140. https://doi.org/10.1080/17499518.2013.871189.

[43] B.M. Das, Principles of Foundation Engineering, Cengage Learning, 2010. https://books.google.com.tr/books?id=v3Mq9szzE1YC.

[44] D.P. Coduto, Foundation Design: Principles and Practices, Pearson Education, 2015. https://books.google.com.tr/books?id=xa6gBwAAQBAJ.

[45] P.G. Constantine, Random Field Simulation (https://www.mathworks.com/matlabcentral/fileexchange/27613-random-field-simulation), (2020).

[46] A.W. Stuedlein, S.L. Kramer, P. Arduino, R.D. Holtz, Geotechnical Characterization and Random Field Modeling of Desiccated Clay, J. Geotech. Geoenvironmental Eng. 138 (2012) 1301–1313. https://doi.org/10.1061/(asce)gt.1943-5606.0000723.

[47] P.K. Robertson, K.L. Cabal, Guide to Cone Penetration Testing for Geotechnical Engineering, California, 2015.

[48] P.K. Robertson, R.G. Campanella, Interpretation of cone penetration tests. Part II: clay., Can. Geotech. J. 20 (1983) 734–745. https://doi.org/10.1139/t83-079.

[49] K. Senneset, R. Sandven, N. Janbu, Evaluation of soil parameters from piezocone tests, Transp. Res. Rec. (1989) 24–37.

[50] JCSS, Probabilistic Model Code Part 1 - Basis of Design, Joint Committee of Structural Safety, 2001.